J Biol Inorg Chem (2002) 7: 37–45
DOI 10.1007/s007750100263

ORIGINAL ARTICLE

**E. Krahn · B.J.R. Weiss · M. Kröckel · J. Groppe
G. Henkel · S.P. Cramer · A.X. Trautwein
K. Schneider · A. Müller**

The Fe-only nitrogenase from *Rhodobacter capsulatus*: identification of the cofactor, an unusual, high-nuclearity iron-sulfur cluster, by Fe *K*-edge EXAFS and ^{57}Fe Mössbauer spectroscopy

Received: 9 April 2001 / Accepted: 22 May 2001 / Published online: 4 July 2001

Abstract Samples of the dithionite-reduced FeFe protein (the dinitrogenase component of the Fe-only nitrogenase) from *Rhodobacter capsulatus* have been investigated by ^{57}Fe Mössbauer spectroscopy and by Fe and Zn EXAFS as well as XANES spectroscopy. The analyses were performed on the basis of data known for the FeMo cofactor and the P cluster of Mo nitrogenases. The prominent Fourier transform peaks of the Fe *K*-edge spectrum are assigned to Fe-S and Fe-Fe interactions at distances of 2.29 Å and 2.63 Å, respectively. A significant contribution to the Fe EXAFS must be assigned to an Fe backscatterer shell at 3.68 Å, which is an unprecedented feature of the trigonal prismatic arrangement of iron atoms found in the FeMo cofactor of nitrogenase MoFe protein crystal structures. Additional Fe···Fe interactions at 2.92 Å and 4.05 Å clearly indicate that the principal geometry of the P cluster is also conserved. Mössbauer spectra of ^{57}Fe-enriched FeFe protein preparations were recorded at 77 K (20 mT) and 4.2 K (20 mT, 6.2 T), whereby the 4.2 K high-field spectrum clearly demonstrates that the cofactor of the Fe-only nitrogenase (FeFe cofactor) is diamagnetic in the dithionite-reduced (''as isolated'') state. The evaluation of the 77 K spectrum is in agreement with the assumption that this cofactor contains eight Fe atoms. In the literature, several genetic and biochemical lines of evidence are presented pointing to a significant structural similarity of the FeFe, the FeMo and and the FeV cofactors. The data reported here provide the first spectroscopic evidence for a structural homology of the FeFe cofactor to the heterometal-containing cofactors, thus substantiating that the FeFe cofactor is the largest iron-sulfur cluster so far found in nature.

Keywords *Rhodobacter capsulatus* · Fe nitrogenase · FeFe cofactor · Mössbauer spectroscopy · Extended X-ray absorption fine structure

Dedicated to Prof. Dr. Philipp Gütlich on the occasion of his 65th birthday

E. Krahn · K. Schneider · A. Müller (✉)
Fakultät für Chemie, Lehrstuhl für Anorganische Chemie I der Universität, Postfach 100131, 33501 Bielefeld, Germany
E-mail: a.mueller@uni-bielefeld.de
Tel.: +49-521-1066153
Fax: +49-521-1066003

B.J.R. Weiss · S.P. Cramer
Department of Applied Science, University of California, Davis, CA 95616, USA

M. Kröckel · A.X. Trautwein
Institut für Physik, Medizinische Universität zu Lübeck, Ratzeburger Allee 160, 23538 Lubeck, Germany

J. Groppe · G. Henkel
Institut für Synthesechemie der Universität, Lotharstrasse 1, 57057 Duisburg, Germany

Introduction

Iron-sulfur clusters belong to the most versatile, multipurpose prosthetic groups in biology. They generally facilitate electron transfer reactions and can act as catalytic centers and intracellular sensors for iron or oxygen [1]. Until now, the largest native metal-sulfur clusters to be characterized have been the P clusters (Fe_8S_7) and the FeMo or FeV cofactors (MFe_7S_9, M = Mo, V) of the nitrogenases. The paradigm that biological nitrogen fixation is dependent on molybdenum was established more than 60 years ago [2, 3] and probably prevented the investigation of other clusters related to this process. Although evidence for the existence of non-Mo nitrogenases was presented early on [4], it was often disregarded. The situation changed with the discovery and isolation of two molybdenum-independent nitrogenase systems in *Azotobacter vinelandii*: a V-dependent nitrogenase only expressed under Mo-deficient conditions, and an Fe-only nitrogenase that is only formed when both Mo and V concentrations are extremely low. These ''alternative'' nitrogenases were then also found in other nitrogen fixing bacteria, and they have provided an exciting new terrain of nitrogenase research. To date, the V

nitrogenases from *A. vinelandii* and *A. croococcum* and the Fe-only nitrogenases of *A. vinelandii*, *Rhodobacter capsulatus* and *Rhodospirillum rubrum* have been isolated and biochemically characterized [5]. Alternative nitrogenases may have technological applications owing to their high rates of hydrogen formation by proton reduction [6].

The conventional, molybdenum-containing nitrogenases, found in all diazotrophs, consist of two independently purifiable protein components. The Fe protein, a homodimer that contains an Fe_4S_4 cluster, transfers electrons in an ATP-dependent process specifically to the MoFe protein. The detailed structures of the *A. vinelandii* and *Clostridium pasteurianum* MoFe proteins have been revealed by X-ray crystal structure analysis [7, 8, 9, 10, 11, 12, 13]. They exhibit an $\alpha_2\beta_2$ tetrameric structure and contain two pairs of metal centers, the P clusters and the FeMo cofactor centers. The P clusters (Fe_8S_7) [12] presumably transfer electrons to the FeMo cofactors ($MoFe_7S_9$); the FeMo cofactors are almost certainly the sites of dinitrogen binding and reduction. The recent crystal structure of the Fe protein/MoFe protein complex supports this electron transfer scheme [13]. The structures of both cluster types are shown in Scheme 1.

The FeMo cofactor is located in the α-subunit and is covalently linked to the protein by a cysteine and a histidine residue. In addition, several hydrogen bonds exist between the protein and various sulfur ligands of the cofactor. Crystallography and EXAFS [14] have identified two characteristic Fe-Fe distances: relatively short 2.6 Å Fe-Fe nearest neighbors, and long 3.7 Å vectors across the prism.

The P clusters are found between the α- and the β-subunits and are linked by three cysteine residues to each subunit [12]. The VFe proteins have not yet been studied by X-ray crystallography but by EXAFS [14, 15, 16, 17] and Mössbauer spectroscopy [18]. The data indicate that the structures of the metal clusters are similar to those of the Mo nitrogenases, with a V atom at the site being occupied by Mo in the FeMo cofactor. In contrast, structural information on the metal clusters of Fe-only nitrogenases by spectroscopic methods is so far lacking. There are, however, genetic and biochemical indications that the FeFe cofactor (FeFeco) is structurally very similar to the FeMo cofactor (FeMoco) and FeV cofactor (FeVco) [19, 20, 21, 22, 23].

The existence of an iron-only nitrogenase system, only expressed if the ambient Mo concentration is extremely low, has been demonstrated in *R. capsulatus* [24, 25]. A rapid and gentle isolation procedure yielding highly active protein components (FeFe protein and Fe protein) has recently been established [26], and the biochemical and EPR spectroscopic properties of this enzyme have been extensively studied [27]. Metal analyses yielded 26 ± 4 Fe atoms per FeFe protein molecule. For other transition metals, including Mo and V, values below 0.1 atoms per molecule have been determined, proving unequivocally that this protein does not contain a FeMo or FeV cofactor. Only zinc was found in higher than trace amounts: values of about 2 atoms per molecule were reported [24].

In this work we present Fe and Zn X-ray absorption and ^{57}Fe Mössbauer data on the FeFe protein from *R. capsulatus*, which prove the existence of a novel binary iron-sulfur cluster showing the highest nuclearity of all members of this intriguing cluster family.

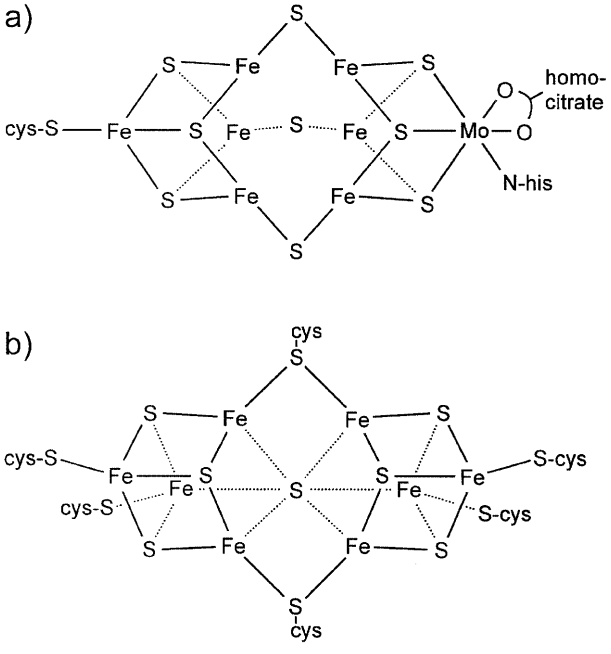

Scheme 1 Schematic representation of **a** the FeMo cofactor and **b** the P cluster structures according to single-crystal X-ray structure analyses of MoFe proteins

Materials and methods

Bacterial strain and growth conditions

The bacterial strain used in this study was a gentamycin- and kanamycin-resistant double mutant of *Rhodobacter capsulatus* strain B10S with a *nifHDK* deletion [24, 25] and an additional deletion in the *modABCD* region. The latter deletion inactivates a high-affinity molybdenum transport system [28]. Cells were grown as described [27]. Only the Fe-citrate stock solution was purified by the active carbon method [29]; L-lactic acid was used in suprapure grade (Sigma).

For the isolation of ^{57}Fe-enriched FeFe protein, an ^{57}Fe-citrate stock solution was prepared by dissolving 100.4 mg (1.76 mmol) ^{57}Fe metal (95.2% ^{57}Fe, Medgenix) in 5 mL concentrated HCl (suprapure grade) at 70 °C. Evaporation to dryness at room temperature yielded yellow crystals, which were dissolved in 5 mL of doubly distilled water. Then 17.6 mL of a 100 mM citric acid solution were added and the pH value was adjusted to 2.5 with NaOH (suprapure grade). An active charcoal suspension (12 mL) [29] was boiled for 20 min and added to the ^{57}Fe solution. After stirring overnight, the active charcoal was removed by filtration. Cells were first grown in a medium containing 1 mM ^{57}Fe-citrate. Each 30 mL of this cell suspension was transferred into 500-mL culture bottles with medium containing 80 μM ^{57}Fe, resulting in a

final ^{57}Fe concentration of about 135 μM. For maximal derepression, Fe concentrations of 500–1000 μM were found to be optimal [24]. Cells were incubated in the light for about 24 h.

Sample preparation

The isolation of the protein components, determination of the protein content, and the activity measurements were completed as described before [27].

For Mössbauer spectroscopy, 800 μL of a solution of as-purified ^{57}Fe-enriched FeFe protein and 600 μL of an independently prepared sample that was supplied with an excess of dithionite and methyl viologen as redox mediator (final concentrations of 10 mM and 0.25%, respectively) were loaded by a gas-tight syringe into cylinder-shaped sample cells of 1 cm diameter and subsequently stored in liquid nitrogen. Protein concentrations were 12 mg mL^{-1} and specific activities (acetylene reduction)[1] about 50 nmol ethylene formed mg^{-1} min^{-1}.

For EXAFS spectroscopy, the solution of the purified FeFe protein was concentrated to a final volume of about 150 μL in a Minicon B15 chamber (Amicon). The protein content was determined to be 150 mg mL^{-1} and the specific activity was 140 nmol ethylene formed mg^{-1} min^{-1}. The sample was loaded with a gas-tight syringe into a lucite sample cell with windows sealed with Kapton tape. The filled cell was subsequently stored in liquid nitrogen.

Mössbauer measurements

Mössbauer spectra were recorded with a conventional constant-acceleration spectrometer using a 1.85 GBq ^{57}Co source in a Rh matrix. Measurements at 4.2 and 77 K were performed using a bath cryostat (VariOx 306, Oxford Instruments) with a permanent magnet mounted outside the cryostat producing a field of 20 mT. High-field measurements (6.2 T) were performed within a cryostat equipped with a superconducting magnet (Oxford Instruments). The spectra were analyzed assuming Lorentzian lineshape; the isomer shift is quoted relative to α-Fe at room temperature.

EXAFS measurements

Fluorescence-detected X-ray absorption spectra for the FeFe protein samples from Fe and Zn edges were recorded on SSRL beamline 7-3 using Si(220) monochromator crystals. During the measurement the samples were maintained at 14 K in an Oxford CF1208 liquid helium cooled cryostat. The fluorescence was collected by a 13-element Ge detector [30]. Concurrently, the calibration was measured in transmission using two nitrogen-filled ion chambers flanking a metal foil, with the first inflection points defined as 7111.3 and 9659.0 eV for Fe and Zn, respectively. The Fe data include an average of 40 scans per sample on each of two separate data collection trips, while the Zn data represents a single collection of 31 scans. Each scan took about 30 min, and upstream slits reduced the beam spot size on the sample to approximately 2×5 mm. The count rates per array element were maintained below 80 kHz with shaping times of 0.125 μs, and the beam was detuned by 40–50% to reduce harmonics.

EXAFS data analysis

A comparison of the first and last scans indicated no change in the sample over the course of the experiment. Data points were interpolated onto a 0.05 eV grid in energy, then averaged together and converted to k-space where $E_0 = 7131$ eV was used for Fe and 9680 eV for Zn. EXAFS from the averaged data files were extracted using conventional methods [31] and fitted using the Cerius^2 EXAFS module from Molecular Simulations, which incorporates EXCURV92 for EXAFS fitting [32]. This procedure was successfully applied to the *A. vinelandii* MoFe protein [33].

[1]Since the FeFe protein activity was not analyzed at saturating amounts of Fe protein, the maximum activity can be extrapolated to be about 20–50% higher

Results and discussion

Preceding investigations had yielded striking biochemical and genetic evidence pointing to a strong structural similarity of the FeMo cofactor and the cofactor of the iron-only nitrogenase:

1. Under in vivo conditions the cofactor of the Fe nitrogenase can be replaced by the conventional FeMo cofactor, forming a hybrid enzyme [19, 20], and vice versa; the FeMoco-deficient apoprotein can be successfully reconstituted and activated with the iron-only cofactor under in vitro conditions [21].
2. The FeMoco is covalently anchored in the MoFe protein through a cysteine and a histidine residue, coordinating to the two terminal atoms (the Mo and the cysteine-bound Fe atom, see Scheme 1a) of the cofactor. These amino acid residues are also conserved in Fe-only nitrogenases (FeFe proteins), as judged by sequence comparisons [5, 25]. Although the MoFe protein and the FeFe protein, both from *R. capsulatus*, are serologically not related [27] and the sequence similarity between their α-subunits is, in total, relatively low (only 26% identity), the location of the two relevant amino acids binding to the cofactors is identical (cysteine at the sequence position 290 and histidine at the position 456 in the α-subunits of both proteins) [25].
3. The *nif*V-encoded protein, a homocitrate synthetase, has been shown to be necessary for both the biosynthesis of the FeMo cofactor and the biosynthesis of the heterometal-free cofactor [20]. *nif*HDK$^-$ *nif*V$^-$ double mutants are unable to grow under N_2-fixing conditions. The Fe nitrogenase, formed in such mutants (during growth with serine as the N source) does not reduce N_2 and reduces C_2H_2 with only extremely low rates [34]. These observations prove that homocitrate is also a catalytically essential component for the iron-only cofactor.
4. A further *nif* gene, *nif*B, has been demonstrated to be required for the biosynthesis of both cofactors [20]. *nif*B encodes a protein that is responsible for the synthesis of an FeS cluster designated as "NifB cofactor". This NifB cofactor is discussed to be a common, heterometal-free intermediate in the biosynthetic pathway of all types of nitrogenase cofactors [5]. *nif*B$^-$ mutants generally produce cofactorless, inactive apo-dinitrogenase components.

Already it appears, from the data listed here, that the FeMo cofactor and the FeFe cofactor should be isostructural cofactors. The intention therefore was to find out whether the postulated structural homology of the

two cofactors can be manifested by Mössbauer and EXAFS techniques, or whether controversial data become obvious pointing to some structural deviations.

Mössbauer spectra of the FeFe protein

Mössbauer spectra of the ^{57}Fe-enriched FeFe protein from *R. capsulatus* were recorded for an as-isolated sample and for a sample to which an excess of dithionite and methyl viologen had been added. Both samples gave identical spectra. Figure 1a shows the Mössbauer spectrum of the as-isolated FeFe protein recorded at 77 K. The spectrum recorded at 4.2 K, in the presence of a magnetic field of 20 mT applied perpendicular to the photon beam, is practically identical (not shown), suggesting an integer-spin ground state for both the FeFeco and the P cluster in the dithionite-reduced state.

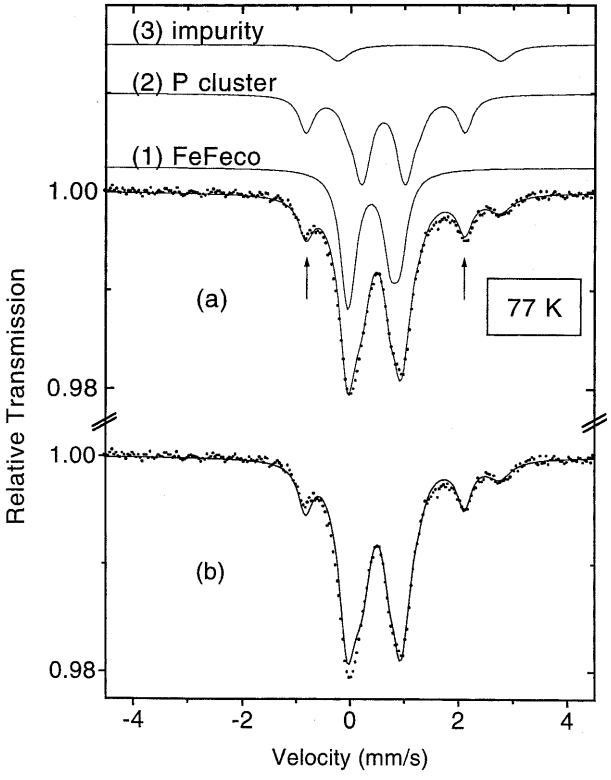

Fig. 1a, b Mössbauer spectra of the FeFe protein of *R. capsulatus* at 77 K. The solid line in **a** is a simulation which represents the superposition of three subspectra shown on top of the spectrum: (*1*) FeFeco (46%), (*2*) P cluster (46%), and (*3*) ferrous impurity (8%). The parameters used are listed in Table 1. *Arrows* indicate the two resolved lines of the "Fe^{2+}" spectral component originating from the P cluster. For comparison, the *solid line* in **b** is a simulation with contributions from the FeFeco (39.5%), the P cluster (52.5%), and the ferrous impurity (8%), keeping all other parameters the same as in **a**

The spectrum at 77 K has been simulated by the superposition of three components assuming the same Lamb-Mössbauer factor: (1) the FeFe cofactor, (2) the P cluster and (3) a ferrous high-spin impurity. The parameters used are summarized in Table 1, and a simulation of the total spectrum is plotted as a solid line in Fig. 1a.

Owing to the complexity of the spectrum and the large number of iron atoms contributing to the overall absorption pattern, it was necessary to assume that the P cluster of the FeFe protein yields the same spectrum as the P cluster of the MoFe protein. This assumption was based on the fact that the only two absorption lines, which are clearly resolved in the spectrum (see arrows in Fig. 1), have parameters almost identical to those reported for the Fe^{2+} component of the P cluster in the MoFe protein of *K. pneumoniae* [35], indicating structural similarity (if not identity) of the P cluster in the FeFe protein with that of the MoFe protein [35, 36] as well as that of the VFe protein [18]. This assumption is corroborated by the fact that the six cysteine residues, connecting the P clusters covalently to the MoFe protein, are conserved in the alternative nitrogenases [5]. In strict analogy to the MoFe protein, of the six cysteines which are suggested to function as ligands of the P cluster in the iron-only nitrogenase of *R. capsulatus*, three are located in the α-subunit (at the amino acid sequence positions 78, 103 and 169) and three in the β-subunit (at the positions 70, 95 and 153) of the FeFe protein component [25]. The contribution of the P cluster (2) to the total absorption area in Fig. 1 is ca. 46% and was obtained by fitting the intensity of the Fe^{2+} subspectrum while fixing the intensity ratio of the Fe^{2+}, S and D components. The iron impurity (3), also reported to be present in V nitrogenase preparations

Table 1 Mössbauer parameters at 77 K

Origin	Spectral component	δ (mm/s)	ΔE_Q (mm/s)	Γ	η[b]	Area (%)	Number of sites
P cluster	Fe^{2+}	0.64(1)	2.94(1)	0.32[c]	0.0(3)	11.5[d]	2[a]
	S	0.61[a]	1.34[a]	0.32[c]	0.0(3)	5.7[d]	1[a]
	D_1	0.61[a]	0.90[a]	0.32[c]	1.0(3)	28.8[d]	5[a]
	D_2	0.61[a]	0.73[a]	0.32[c]	1.0(3)		
FeFeco	M_1	0.37(2)	0.74(2)	0.32[c]	0.5(3)	23.0[e]	8
	M_2	0.42(2)	1.00(2)	0.32[c]	0.5(3)	23.0[e]	–
Impurity	Fe^{2+}	1.26(1)	3.00(1)	0.5	–	8.0	–

[a]Values from [34]
[b]Obtained from the 4.2 K spectrum in a field of 6.2 T applied parallel to the photon beam
[c]Kept fixed at these values
[d]Ratios chosen to give the correct number of sites for the P cluster
[e]Area ratios of the two subspectra chosen arbitrarily

from *A. vinelandii* [18], accounts for ca. 8% of the total absorption area. The absorption peak at 2.8 mm/s is attributed to the high-energy line of the quadrupole doublet of this iron impurity. Its isomer shift ($\delta = 1.26$ mm/s) is typical for the ferrous high-spin state of a hexacoordinated iron species with an oxygen and/or nitrogen ligand sphere. Isomer shift as well as quadrupole splitting of this species are not very specific, because they are typical for many ferrous salts and complexes.

The remaining part of the spectrum, an asymmetric doublet (1), is ascribed to the FeFeco. It was fitted with two doublets of equal intensity (designated M_1 and M_2 in Table 1). The asymmetry of this doublet indicates that at least two different kinds of iron sites constitute the FeFeco signal. The choice of equal intensities for the two subspectra M_1 and M_2 is rather arbitrary and only due to the lack of better spectral resolution. Like the P cluster, the FeFeco signals account for 46% of the total absorption area, indicating an identical number of Fe sites in both clusters. The isomer shifts and quadrupole splittings of the FeMoco, FeVco and FeFeco are very similar (Table 2), indicating similar molecular structures in all three cofactors.

Mössbauer spectra were also recorded at 4.2 K in the presence of a strong magnetic field (6.2 T) applied parallel to the photon beam (Fig. 2). The magnetic splitting of the spectrum is only due to the applied field. No additional internal field is observed. Therefore, these data provide unambiguous evidence that both metal clusters (P cluster and FeFeco) are diamagnetic in the as-isolated (dithionite-reduced) state. This result is consistent with the observation that the FeFe protein is EPR silent in this redox state [27]. In the MoFe and the VFe proteins the P clusters are also diamagnetic in the as-isolated form, whereas the FeMo and FeV cofactors are paramagnetic ($S = 3/2$).

In a formal consideration, the FeFeco must contain an even number of Fe^{III} and Fe^{II} sites to account for the observed diamagnetism. Assuming only six Fe atoms in the FeFeco (and eight in the P cluster), the FeFeco signals would account for 39.5% of the total absorption area and the P cluster signals for 52.5%, keeping the impurity iron at 8%. A corresponding simulation of the 77 K spectrum is clearly not in agreement with the experiment around zero velocity (Fig. 1b). From this observation, together with the observed diamagnetism at 4.2 K, the conclusion can be drawn that the FeFeco actually contains eight Fe atoms. The average isomer shift of $\delta_{av} \approx 0.4$ mm/s points to an average oxidation state of 2.5+, indicating that the FeFeco formally consists of four Fe^{II} and four Fe^{III} sites. This view is consistent (1) with the results of semiempirical calculations on the electronic structure of idealized models of the FeMoco, FeVco and FeFeco [37] and (2) with the conclusion recently drawn for the M^N center of the MoFe protein of nitrogenase from *A. vinelandii*: the isomer shifts and the anisotropies of magnetic hyperfine tensors of that protein were rationalized with a model that contains (formally) a $[Mo^{4+}\text{-}4Fe^{2+}\text{-}3Fe^{3+}]$ core [38], with a δ_{av} value of this core being essentially the same as that of the FeFe cofactor.

X-ray absorption studies on the FeFe protein

Analysis of the Fe *K*-edge XAS (Fig. 3) and EXAFS spectra revealed a marked similarity in key features to the respective MoFe protein data. These similarities were evident initially in a comparison of the Fourier transforms shown in Fig. 4. The 2.6 Å Fe-Fe and 3.7 Å Fe-Fe interactions, unique to the structure of the FeMo and FeV cofactors, are retained in the FeFe protein. They are, for instance, distinct from the 2.7 and 3.8 Å Fe-Fe distances characteristic of the prismane-type

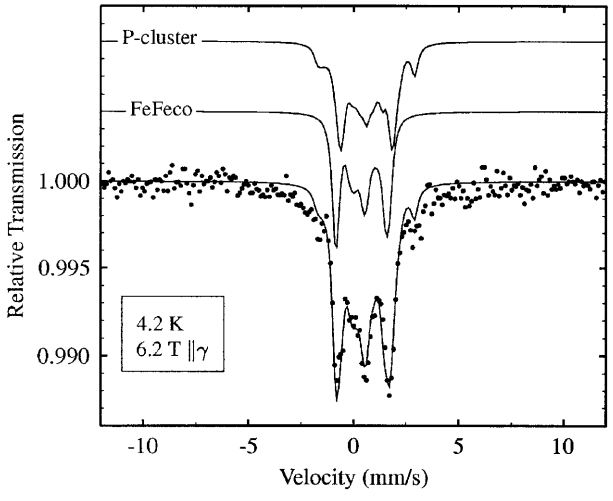

Fig. 2 4.2 K Mössbauer spectrum of the FeFe protein of *R. capsulatus* in a magnetic field of 6.2 T applied parallel to the photon beam. The solid line is a simulation for $S = 0$ with the parameters of the P cluster and of the FeFeco summarized in Table 1. The high-spin ferrous impurity (8% of total area in the 77 K spectrum) is not included in this simulation

Table 2 Isomer shifts and quadrupole splittings of the three cofactors in their respective, dithionite-reduced, dinitrogenase proteins

Cofactor	δ (mm/s)	ΔE_Q (mm/s)	Area (%)	Ref
FeMoco[a]	0.40	0.76	40	[35]
FeVco[a]	0.39	0.94	48	[18]
FeFeco[b]	0.37/0.42[c]	0.74/1.00[c]	46	This work

[a]From *A. vinelandii*
[b]From *R. capsulatus*
[c]Values represent the subspectral components M_1 and M_2 (see Table 1 and text)

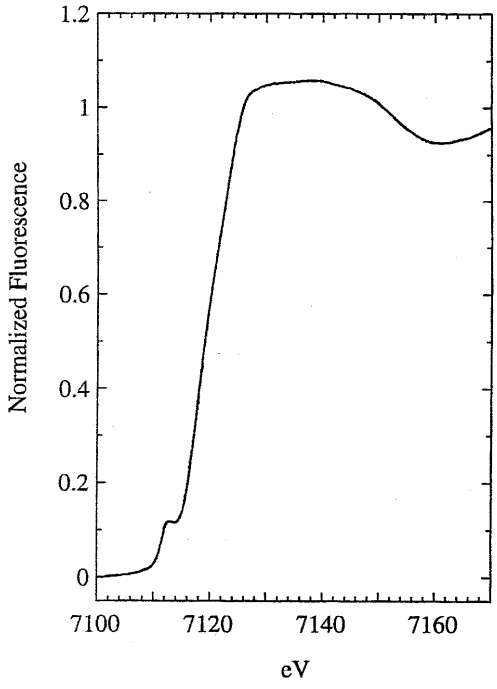

Fig. 3 Fe *K*-edge XAS spectrum of the Fe-only nitrogenase FeFe protein

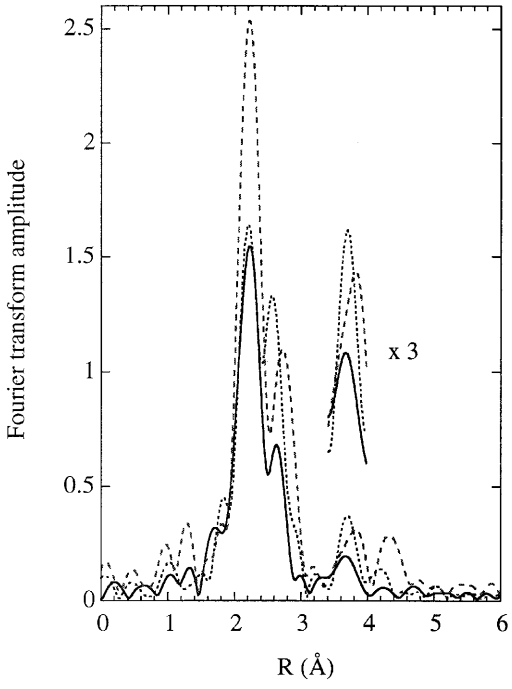

Fig. 4 Fourier transforms of the EXAFS spectra of the Fe-only nitrogenase FeFe protein (*solid line*), the Mo nitrogenase MoFe protein (*dotted line*) and the metal cluster anion $[Fe_6S_6Cl_6]^{3-}$ (*dashed line*), over the range $k = 3.00$–14.75 Å^{-1}

cluster [14] in the Fourier transform which has been integrated in Fig. 4 for comparison. A further significant characteristic of the Fe prismane cluster, the pronounced peak at ca. 4.4 Å in the Fourier transform, has no comparable counterpart in the transforms of the FeFe protein spectra. The 2.3 Å Fe-S distance is present in the MoFe protein and the FeFe protein, as well as in the Fe prismane cluster.

The Fe EXAFS was fitted in the range $k = 2.50$–14.75 Å^{-1} (see Table 3 and Fig. 5), assuming the spectrum to be composed of the backscattered waves of two principal contributors, namely the FeFeco and the P cluster, respectively.

The starting model for the refinement procedure was defined by a shell of four sulfur atoms directly bonded to each iron and a second shell containing three nearest iron neighbors with distances typical for all types of iron-sulfide-thiolate clusters known so far. This incomplete structure was significantly improved by adding a further iron shell at a distance of ca. 3.68 Å (occupancy ca. 1.0), giving a model-independent basis for the following structure expansion process. During this procedure, we used the standard FeMo cofactor model from Kim and Rees [7], assuming the substitution of an Fe atom in place of the Mo center and the revised P cluster model for the nitrogenase MoFe protein [12] to develop the final set of coordination shells necessary to optimize the curve-fitting procedure. All shells together represent the complete set of Fe-Fe and Fe-S interactions within the X-ray models of the MoFe protein. Though the final structure, derived from our EXAFS data, is therefore not completely independent from model considerations, the structural elements typical for a trigonal prismatic arrangement of iron atoms, namely the iron backscatterer shell at 3.68 Å, have been derived from first principles, and each additional component up to a distance limit of 4.8 Å proved to be a significant contribution. During the last stages of the structural refinement procedure, the coordination numbers for each shell of backscatters were fixed at values derived from the structural elements given in Scheme 1a for the FeMoco and in Scheme 1b for the P cluster. The EXAFS function, calculated from the final EXAFS structure, is in excellent agreement with the experimental data. All details relevant to the curve-fitting process are given in Table 3.

Other fits, based on a FeFeco model that contains no Fe atom at the position which is occupied by the molybdenum atom in the FeMoco structure (data not shown), demonstrate that the analysis is not very sensitive to the difference between 15 and 16 Fe atoms. Nevertheless, all fits done show the 3.68 Å Fe-Fe cross-cluster distance which is highly characteristic of trigonal prismatic Fe sites, as they have been described for the FeMo cofactor. The trigonal iron prism can be identified simply by the number of its characteristic Fe-Fe interactions which are associated with the diagonals of its quadratic faces. Within the Fe prism, there are a total of 12 such interactions, whereas within the P cluster only two of these interactions are present. Our analysis is in excellent accordance with a total of 14 such interactions and thus confirms the presence of trigonal prismatic Fe sites. Historically, the 3.7 Å distance was one of the first

Table 3 Curve-fitting parameters for Fe *K*-edge EXAFS of *R. capsulatus* nitrogenase FeFe protein over the range $k = 2.50–14.75$ Å^{-1}. The parameters contain the sum of FeFeco [$Fe_8S_9(S_{cys})L_3$] (L = O, N) and P cluster [$Fe_8S_7(S_{cys})_6$] contributions

	Fe-N/O	Fe-S	Fe-Fe	Fe-Fe	Fe-S	Fe-Fe	Fe-Fe	Fe-S	Fe-Fe	Fe-Fe
R (Å)[a]	2.16	2.29	2.63	2.92	3.59	3.68	4.05	4.20	4.48	4.67
N[b]	0.35	3.56	3.38	0.25	0.75	0.87	0.12	3.18	0.25	0.50
$2\sigma^2$ (Å^2)	0.002	0.012	0.027	0.001	0.010	0.009	0.002	0.080	0.002	0.010

[a]The R factor is determined to $R = 10.98$, calculated according to: $R = \sum_i^N \left(k_i^3 \Big/ \sum_j^N k_j^3 |\chi^{expt}(k_j)| \right) \left(|\chi^{expt}(k_i) - \chi^{th}(k_i)| \right) \times 100\%$
[b]N = number of data points

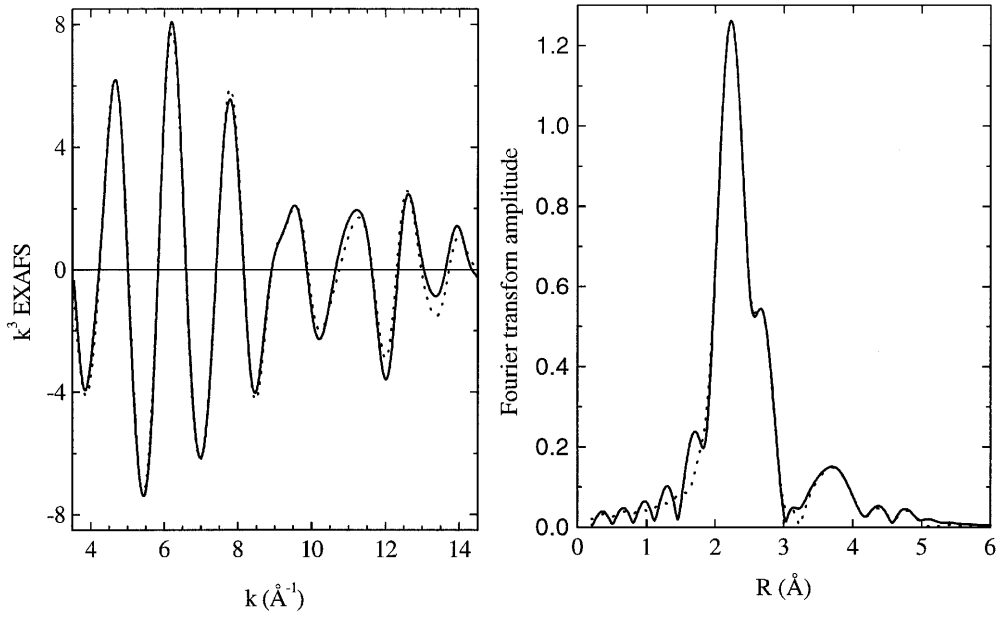

Fig. 5 Fe *K*-edge EXAFS (*left spectrum*) and Fourier transforms (*right spectrum*) of the Fe-only nitrogenase FeFe protein (*solid line*) and a fit (*dotted line*) analyzed over the range $k = 2.50–14.75$ Å^{-1}

clues to the FeMo cofactor structure prior to the discovery and differentiation of the P cluster [39].

Considerations on the chemical behavior of zinc could not rule out a putative FeZn cofactor: the existence of heterocubane cluster centers of the type $[Fe_3S_4Zn]^{n+}$, which were generated in low molecular weight compounds as well as in proteins (reviewed in [40]), shows that zinc has a tendency to be captured by the three μ_2-S atoms from an $Fe_3(\mu_2\text{-}S)_3$ fragment as it is present in the cofactor (discussed in [41]). Corresponding Mo and V heterocubane clusters serve as important model compounds for the FeMo and FeV cofactors.

Zn EXAFS were fitted over the range $k = 3.00–13.00$ Å^{-1} using N, R and σ^2 values for Zn-N and Zn-S interactions. The Zn *K*-edge EXAFS data verify that Zn, which was the only transition element except for Fe found to be present in relatively high amounts (1–2 atoms per protein molecule) in FeFe protein preparations [27], has not been substituted for Mo in the Fe-only protein. Also the Zn EXAFS Fourier transform (Fig. 6) provides evidence against the possibility of a Zn-Fe interaction, particularly at the 2.6 Å distance expected in the case of Zn occupying the "Mo position". The first peak fits with two Zn-N interactions, while the second peak, a possible candidate for Zn-metal interaction, is at a distance of 2.3 Å, which is far too short for the end metal distance to Fe in a putative FeZn cofactor, and fits roughly to two Zn-S interactions. As is evident from both the analysis and Fourier transform, 2.6 Å Zn-Fe interactions will not fit the data, and it is possible that Zn is bound to cysteinyl residues elsewhere in the protein.

Conclusions

From our spectroscopic results, together with the already discussed data obtained from the biochemical investigations and genetic analyses of nitrogenase systems, it can be concluded that the FeMo cofactor and the heterometal-free cofactor of the Fe nitrogenase are structurely homologous and that the only fundamental structural difference between the two cofactors is an additional iron atom replacing the molybdenum atom in the Fe nitrogenase cofactor.

The analysis of the Fe EXAFS data provides strong evidence that the main structural element of the Fe-Moco, the central trigonal prismatic arrangement of Fe atoms, is also present in the FeFeco (Scheme 2b). This structural element is so far unprecedented in synthetic chemistry [41]. The two terminal atoms, by which the FeMo cofactor is anchored in the protein, are the

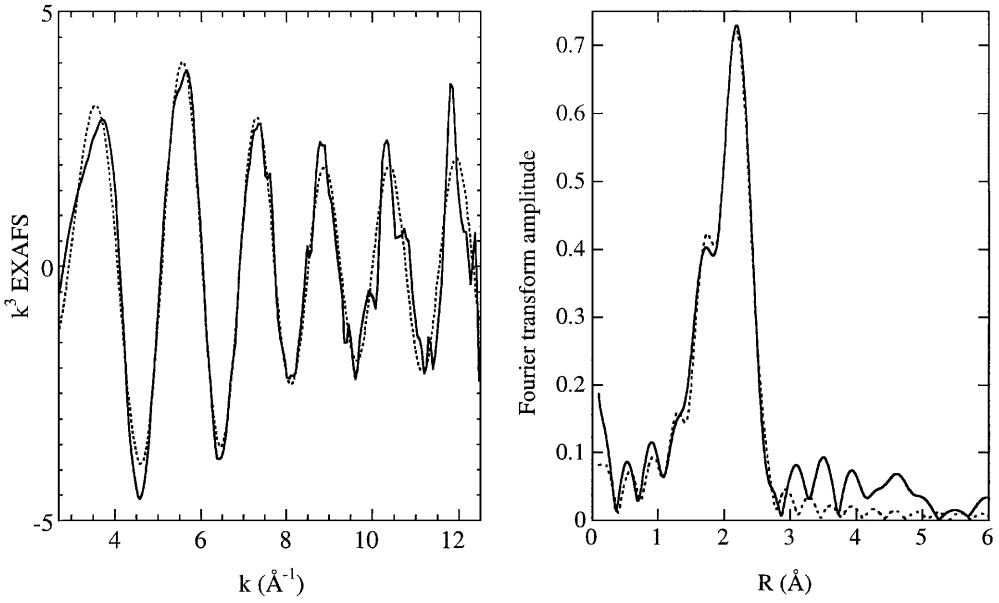

Fig. 6 Zn *K*-edge EXAFS (*left spectrum*) and Fourier transforms (*right spectrum*) of the Fe-only nitrogenase FeFe protein (*solid line*) and a fit (*dotted line*) with two 2.02 Å Zn-N ligands and two 2.33 Å Zn-S ligands

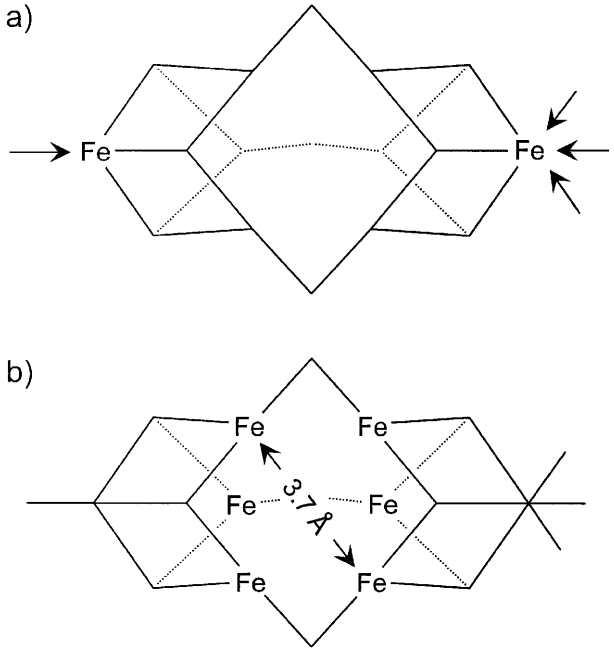

Scheme 2 Structural elements of the FeFe cofactor: **a** terminal Fe positions determined by constraints of the cofactor binding site within the protein; **b** trigonal prismatic arrangement of Fe atoms indicated to be present according to the FeFe protein EXAFS data

cysteine-bound Fe atom and the histidine-bound Mo atom (Scheme 1a). In the case of the heterometal-free cofactor, the two protein-anchoring atoms are both Fe atoms which have to be present at the positions as indicated in Scheme 2a.

The Mössbauer data are in agreement with the presence of eight Fe atoms since they show that the iron-only cofactor is diamagnetic and contributes 50% to the total absorption area attributed to originate from the cluster centers. Formally this type of cofactor consists of four Fe^{II} and four Fe^{III} sites.

Our findings substantiate (1) that the cofactor of the Fe-only nitrogenase in *R. capsulatus* deserves the designation "FeFe cofactor", implying structural homology to the FeMo and FeV cofactors, and (2) that binding and reduction of nitrogen can be catalysed (based solely on Fe) by this unusual and so far largest member of the family of naturally occurring iron-sulfur clusters.

Acknowledgements We thank Prof. W. Klipp for providing the bacterial strain, Prof. D. Coucouvanis for discussions and the Deutsche Forschungsgemeinschaft for financial support. Support from the U.S. Department of Agriculture, grant no. CSREES 96-3505-3541, is gratefully acknowledged by S.P.C. Stanford Synchrotron Radiation Laboratory is supported by the U.S. Department of Energy, Office of Health and Environmental Research and Office of Basic Energy Science, Divisions of Chemical and Materials Science, and by the National Institute of Health, Biomedical Research Technology Program.

References

1. Beinert H, Holm R, Münck E (1997) Science 277:653–659
2. Bortels H (1930) Arch Mikrobiol 1:333
3. Bortels H (1936/37) Zentralbl Bakteriol Abt II 95:193–218
4. Bishop PE, Jarlenski DML, Hetherington DR (1980) Proc Natl Acad Sci USA 77:7342–7346
5. Eady RR (1996) Chem Rev 96:3013–3030
6. Krahn E, Schneider K, Müller A (1996) Appl Microbiol Biotechnol 46:285–290
7. Kim J, Rees DC (1992) Science 257:1677–1682
8. Bolin JT, Campobasso N, Muchmore SW, Minor W, Morgan TV, Mortenson LE (1993) In: Palacios R, Mora J, Newton WE (eds) New horizons in nitrogen fixation. Kluwer, Dordrecht, pp 89–94
9. Bolin JT, Campobasso N, Muchmore SW, Morgan TV, Mortenson LE (1993) In: Stiefel EI, Coucouvanis D, Newton WE (eds) Molybdenum enzymes, cofactors and model systems. (ACS symposium series 535) American Chemical Society, Washington, pp 186–195

10. Chan MK, Kim J, Rees DC, (1993) Science 260:792–794
11. Rees DC, Chan MK, Kim J (1993) Adv Inorg Chem 40:89–119
12. Peters JW, Stowell MHB, Soltis SM, Finnegan MG, Johnson MK, Rees DC (1997) Biochemistry 36:1181–1187
13. Schindelin H, Kisker C, Schlessman JL, Howard JB, Rees DC (1997) Nature 387:370–376
14. Chen J, Christiansen J, Tittsworth RC, Hales BJ, George SJ, Coucouvanis D, Cramer SP (1993) J Am Chem Soc 115:5509–5515
15. Arber JM, Dobson BR, Eady RR, Hasnain SS, Garner CD, Matsushita T, Nomura M, Smith BE (1989) Biochem J 258:733–737
16. George GN, Coyle CL, Hales BJ, Cramer SP (1988) J Am Chem Soc 110:4057–4059
17. Harvey I, Arber JM, Eady RR, Smith BE, Garner CD, Hasnain SS (1990) Biochem J 266:929–931
18. Ravi N, Moore V, Lloyd SG, Hales BJ, Huynh BH (1994) J Biol Chem 269:20920–20924
19. Gollan U, Schneider K, Müller A, Schüddekopf K, Klipp W (1993) Eur J Biochem 215:25–35
20. Pau RN, Eldridge ME, Lowe DJ, Mitchenall LA, Eady RR (1993) Biochem J 293:101–107
21. Davis R, Lehman L, Petrovich R, Shah VK, Roberts GP, Ludden PW (1996) J Bacteriol 178:1445–1450
22. Moore VG, Tittsworth RC, Hales BJ (1994) J Am Chem Soc 116:12101–12102
23. Smith BE, Eady RR, Lowe DJ, Gormal C (1988) Biochem J 250:299–302
24. Schneider K, Müller A, Schramm U, Klipp W (1991) Eur J Biochem 195:653–661
25. Schüddekopf K, Hennecke S, Liese U, Kutsche M, Klipp W (1993) Mol Microbiol 8:673–684
26. Schneider K, Gollan U, Selsemeyer-Voigt S, Plass W, Müller A (1994) Naturwissenschaften 81:405–408
27. Schneider K, Gollan U, Dröttboom M, Selsemeier-Voigt S, Müller A (1997) Eur J Biochem 244:789–800
28. Wang G, Angermüller S, Klipp W (1993) J Bacteriol 175:3031–3042
29. Schneider K, Müller A, Johannes KU, Diemann E, Kottmann J (1991) Anal Biochem 193:292–298
30. Cramer SP, Tench O, Yocum M, George GN (1988) Nucl Instrum Methods A 266:586–591
31. Cramer SP, Hodgson KO, Stiefel EI, Newton WE (1978) J Am Chem Soc 100:2748–2760
32. BIOSYM/Molecular Simulations (1995) EXAFS. In: Computational instruments diffraction and microscopy user's reference. BIOSYM/Molecular Simulations, San Diego, pp 233–347
33. Christiansen J, Tittsworth RC, Hales BJ, Cramer SP (1995) J Am Chem Soc 117:10017–10024
34. Dröttboom M (1998) Dissertation, University of Bielefeld, Germany
35. McLean PA, Papaeftymiou V, Orme-Johnson WH, Münck E (1987) J Biol Chem 262:12900–12903
36. Huynh BH, Henzl MT, Christner JA, Zimmermann R, Orme-Johnson WH, Münck E (1980) Biochim Biophys Acta 623:124–138
37. Plass W (1994) J Mol Struct (Theochem) 315:53–62
38. Yoo SJ, Angore HC, Papaefthymiou V, Burgess BK, Münk E (2000) J Am Chem Soc 122:4926–4936
39. Arber JM, Flood AC, Garner CD, Gormal CA, Hasnain SS, Smith BE (1988) Biochem J 252:421–425
40. Holm RH (1992) Adv Inorg Chem 38:1–71
41. Müller A, Krahn E (1995) Angew Chem Int Ed Engl 34:1071–1078